Bull Volcanol (1998) 59:262–275

ORIGINAL PAPER

R. S. Fiske · K. V. Cashman · A. Shibata · K. Watanabe

Tephra dispersal from Myojinsho, Japan, during its shallow submarine eruption of 1952–1953

Received: 5 December 1996 / Accepted: 17 September 1997

Abstract A new and detailed bathymetric map of the Myojinsho shallow submarine volcano provides a framework to interpret the physical volcanology of its 1952–1953 eruption, especially how the silicic pyroclasts, both primary and reworked, enlarged the volcano and were dispersed into the surrounding marine environment. Myojinsho, 420 km south of Tokyo along the Izu–Ogasawara arc, was the site of approximately 1000 phreatomagmatic explosions during the 12.5-month eruption. These explosions shattered growing dacite domes, producing dense clasts that immediately sank into the sea; minor amounts of pumice floated on the sea surface after some of these events. The Myojinsho cone has slopes of almost precisely 21° in the depth range 300–700 m.We interpret this to be the result of angle-of-repose deposition of submarine pyroclastic gravity flows that traveled downslope in all directions. Many of these gravity flows resulted from explosions and associated dome collapse, but others were likely triggered by the remobilization of debris temporarily deposited on the summit and steep upper slopes of the cone. Tephra was repeatedly carried into air in subaerial eruption columns and fell into the sea within 1–2 km of the volcano's summit, entering water as deep as 400 m. Because the fall velocity of single particles decreased by a factor of ~30 in passing from air into the sea, we expect that the upper part of the water column was repeatedly choked with hyperconcentrations of fallout tephra. Gravitational instabilities within these tephra-choked regions could have formed vertical density currents that descended at velocities greater than those of the individual particles they contained. Upon reaching the sea floor, many of these currents probably continued to move downslope along Myojinsho's submarine slopes. Fine tephra was elutriated from the rubbly summit of the volcano by upwelling plumes of heated seawater that persisted for the entire duration of the eruption. Ocean currents carried this tephra to distal areas, where it presumably forms a pyroclastic component of deep-sea sediment.

Key words Submarine silicic dome · Submarine pyroclastic cone · Shallow submarine eruption · Myojinsho · Submarine pyroclastic gravity flow

Introduction

We focus on the physical volcanology of Myojinsho's 1952–1953 activity, one of the best-documented shallow submarine silicic eruptions of the twentieth century. We review some of the many subaerial observations of this activity, placing them, where possible, in the context of a new bathymetric map. The two main issues we address are: (a) How did the proximal Myojinsho cone grow in 1952–1953? and (b) How did the eruption influence deep-sea sedimentation in distal areas?

Myojinsho's 1952–1953 eruption was small, comparable to the subaerial dome-building eruptions at Unzen, Japan, in 1991–1995 (Sato et al. 1992; Nakada and Fujii 1993; Nakada et al. 1995) and Mount St. Helens in 1980–1986 (Swanson et al. 1987; Swanson and Holcomb 1990). As at these subaerial examples, the Myojinsho eruption was episodic, with dome extrusion, explosions, and associated dome collapse punctuating periods of relative quiescence. Moreover, like subaerial dome-

Editorial responsibility: J. McPhie

Richard S. Fiske (✉)
Smithsonian Institution MRC-119, Washington, DC 20560, USA
Fax: +202 357 2476
e-mail: rfiske@volcano.si.edu

Katharine V. Cashman
Department of Geological Sciences, University of Oregon, Eugene, OR 97403–1272, USA

Atsushi Shibata
Hydrographic Department, Japan Maritime Safety Agency, 3–1 Tsukiji 5-chome, Chuo-ku, Tokyo 104, Japan

Kazuki Watanabe
Hydrographic Department, Japan Maritime Safety Agency, 3–1 Tsukiji 5-chome, Chuo-ku, Tokyo 104, Japan

building eruptions, fragmental deposits produced by the 12.5-month Myojinsho event are the combined result of primary magmatic fragmentation and secondary dome collapse. Although no universally accepted terminology exists for the tephra erupted from shallow submarine volcanoes (and we do not introduce one here), we use *tephra* to describe the debris produced at Myojinsho and *pyroclastic* (in a broad sense) as the descriptive modifier for the numerous gravity flows that likely traveled down its slopes.

No discussion of the 1952–1953 Myojinsho eruption would be complete without acknowledgement of the tragedy that befell the Japanese survey ship No. 5 Kaiyo-maru. At approximately 12:20 p.m. JST on 24 September 1952, the ship approached the temporarily quiescent Myojinsho and was shattered by a large phreatomagmatic explosion, killing all 31 people aboard. This disaster shocked the world and prompted the Japanese Maritime Safety Agency (JMSA) to establish a circular restricted area closed to shipping, centered on Myojinsho and having a radius of 10 nautical miles. This restricted area, still in effect today, has prevented direct study of the Myojinsho cone. However, this tragedy, together with recent deaths caused by dome collapse at Unzen Volcano, Japan, Merapi Volcano, Indonesia, and Soufriere Hills, Montserrat, does underline the importance of understanding these small but relatively frequent dome-producing eruptions.

Finally, deposits similar to those produced at Myojinsho are common in ancient submarine silicic volcanic successions (e.g., Busby-Spera 1988; Cas et al. 1989; Houghton and Landis 1989; Kano 1996; Mueller 1991; Tassé et al. 1978), but in most cases the location of source vents, volcanic edifice configurations, and the relationship of deposits to specific volcanic events are poorly known. At Myojinsho, although safety restrictions prevented dredging and submersible study of the deposits, the configuration of the cone is well known, and its 1952–1953 eruption was carefully observed. Furthermore, interpretation of Myojinsho's 1952–1953 eruption is well constrained by the newly available bathymetry which, together with the subaerial observations, contributes significantly to understanding tephra-dispersal processes operating at explosive submarine volcanoes. Recent studies have shown that a vast field of isolated and overlapping submarine volcanoes (including at least seven silicic calderas) lies along the Izu-Ogasawara arc, but study of this field has barely begun (e.g., Murakami and Ishihara 1985; Yuasa et al. 1991; Fiske and Naka 1994; Fiske et al. 1995). It seems clear, however, that: (a) many aspects of submarine eruption and deposition are significantly different from equivalent subaerial processes, and (b) pyroclastic terminology, including the nuances associated with terms such as pyroclastic, volcaniclastic, and epiclastic, have been strongly influenced by observations made on land. A more complete discussion of terminology will be warranted only when the nature of submarine pyroclastic volcanology is better understood.

Methods

We use written accounts, photographs, and a new high-precision bathymetric map of the Myojinsho area to interpret Myojinsho's 1952–1953 eruption. The written accounts mostly consist of scientific papers and contemporary newspaper articles, most in Japanese. Particularly valuable has been the 112-page report of a committee convened by the Japanese Maritime Safety Agency (JMSA) to investigate the No. 5 Kaiyo-maru disaster (Marine Safety Board 1953). This report describes many aspects of the event not recorded in the literature. We have also studied more than 50 photographs of the eruption taken by scientists, journalists, and military personnel.

Geological setting and eruptive history

Myojinsho lies along the axis of the Izu–Ogasawara arc, approximately 420 km south of Tokyo (Fig. 1). Yuasa et al. (1991) identify 19 volcanoes along the northern part of the arc, extending from Oshima in the north to Kinyo Seamount in the south. Some of these volcanoes have grown above sea level to form islands (e.g., Oshima, Miyakejima, and Aogashima), but most remain below sea level as submarine volcanoes (e.g., Myojin Knoll, Daisan-Sumisu Knoll, and Getsuyo Seamount). At least seven submarine calderas lie along this part of the arc (Murakami and Ishihara 1985), and each has likely been the site of silicic pyroclastic eruptions. For example, the caldera associated with Myojin Knoll, the first of these silicic structures to receive detailed, submersible-based study, was the site of a submarine eruption that produced 35–40 km^3 of rhyolite tephra (Fiske et al. 1995; Naka et al. 1995; Yuasa 1995). The broader volcanologic framework of the Izu–Ogasawara arc has been established by multi-beam sounding surveys (e.g.,

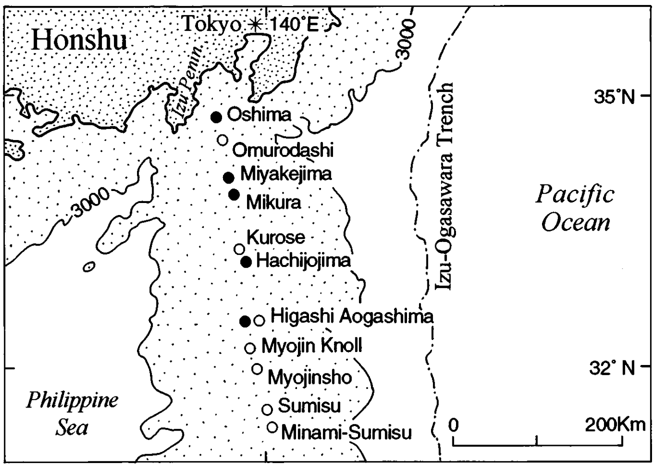

Fig. 1 Location map showing volcanoes along the front of the northern Izu–Ogasawara arc, Japan. *Solid circles* are mafic island volcanoes; *open circles* are submarine calderas

Nagaoka et al. 1991), reconnaissance geologic studies (e.g., Iwabuchi et al. 1994; Takada et al. 1994; Yuasa et al. 1991), and deep-sea drilling (Nishimura et al. 1992).

Pre-eruption bathymetry

The geologic setting and the local bathymetry of Myojinsho were poorly known at the time of the 1952–1953 eruption. A map prepared in 1952 (Fig. 2) showed the volcano to be an elongate, twin-summit edifice located 8–12 km ENE of the Bayonnaise Rocks, jagged spires of hypersthene-augite basalt protruding several meters above sea level (Morimoto et al. 1955). The area of closed contours between the Bayonnaise Rocks and Myojinsho suggested the existence of a caldera, but there was disagreement as to whether Myojinsho was located along the caldera rim (Morimoto and Ossaka 1955) or formed a central cone within the caldera (Dietz and Sheehy 1954).

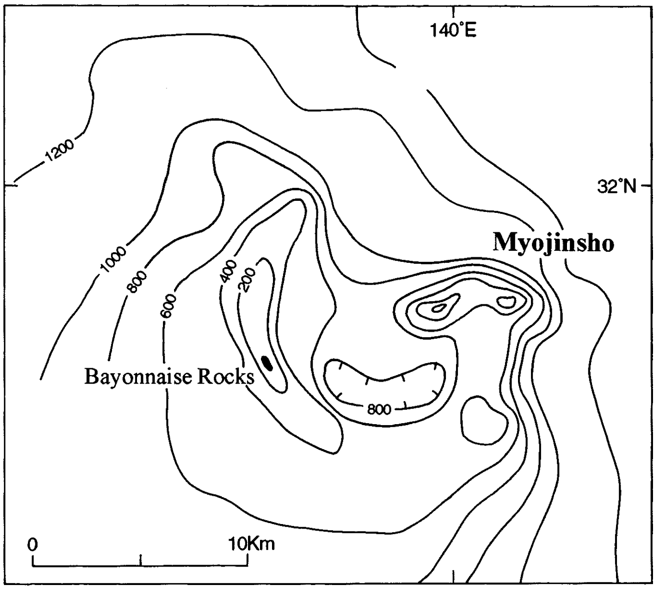

Fig. 2 Pre-1952 bathymetry of the Myojinsho area (modified from Fig. 2 of Morimoto and Ossaka 1955), presented here to show that the local bathymetry was poorly known at the time of the 1952–1953 eruption. Compare this map with the newly available bathymetry, based on a 1989 survey, shown in Fig. 3

1996 bathymetry and generalized geologic history

The bathymetric map of the Myojinsho area (Fig. 3) is the most important new data presented here. Data for this map were gathered by JMSA in 1989. Because of safety considerations, an unmanned, radio-controlled launch was used, enabling the larger survey vessel to remain at a safe distance (Tsukamoto et al. 1990). Published here for the first time, this map is a precise representation of the local Myojinsho bathymetry. The close spacing of the survey lines, many of which are only a few hundred meters apart, implies that the remarkable symmetry of the Myojinsho cone is real and not an artifact of the survey.

The newly prepared bathymetric map (Fig. 3) shows that the Myojinsho cone straddles the rim of a nearly circular caldera 8–9 km in diameter and is clearly a post-caldera feature. At the time of the survey (1989), the summit of the cone was 43 m below sea level.

The caldera floor, at a depth of 1000–1100 m, is dominated by a post-caldera dome complex (and/or pyroclastic cone) approximately 700 m high. Eleven dredge hauls recovered dense lithic clasts from the western slope of the dome complex and the adjacent caldera wall. Five samples analyzed from the dome are

Fig. 3A, B Bathymetry of the Myojinsho area. **A** The symmetrical cone of Myojinsho straddles the northwest rim of an 8 × 10-km caldera. A 700-m-high post-caldera lava dome (and/or flow) complex occupies much of the caldera floor. The contour interval is 50 m in the immediate Myojinsho area and 100 m elsewhere. Simplified from unpublished map prepared by the Hydrographic Department, Japan Maritime Safety Agency; see Fig. 7 for a close-up map of Myojinsho having a 10-m contour interval. **B** Close spacing of track lines along which data were collected near Myojinsho's summit

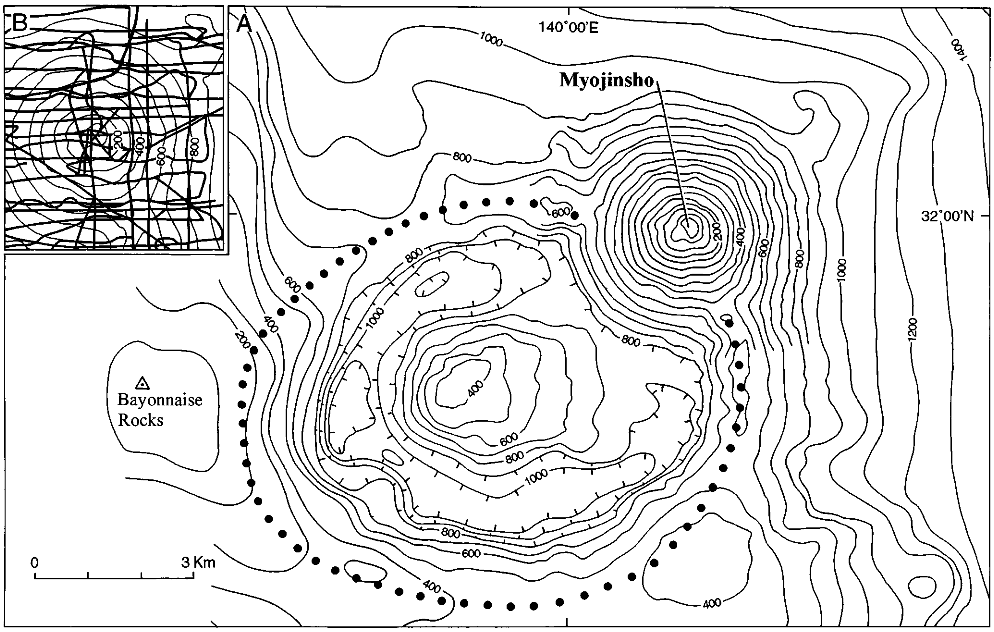

dacite containing 66–69% SiO_2 (Iizasa 1993), and petrographic study of other rocks from the dome and adjacent caldera wall indicates the presence of rocks ranging in composition from andesite to rhyolite (M. Yuasa, pers. commun.).

These and other relationships seen in Fig. 3 suggest the following generalized volcanic history for the Myojinsho area:

1. A cluster of volcanoes grew and coalesced, eventually building a broad edifice more than 20 km in diameter that rose approximately 1200 m above the surrounding sea floor. Scattered bathymetric knolls on this edifice may mark the summits of some of these pre-caldera volcanoes.
2. A caldera formed, probably the result of a large submarine pyroclastic eruption. The present-day caldera (excluding the post-caldera dome complex) has a volume of approximately 25 km^3, but this estimate does not take into account the volume of caldera fill or the missing volcano summit (both of which are unknown). The total volume of caldera collapse might therefore have approached 30–35 km^3, suggesting that more than 60 km^3 of tephra was erupted (assuming an average clast vesicularity of 50%). The existence of a caldera-related pyroclastic deposit has not yet been confirmed.
3. A dome (and/or lava-flow) complex grew on the caldera floor. This imposing feature has a volume of at least 2.6 km^3, nearly 40 times greater than the 1980–1986 dome on the floor of the Mount St. Helens crater (Swanson and Holcomb 1990).
4. Myojinsho grew astride the northeastern caldera rim, and deposits forming its cone mantle both the northeast caldera wall and the nearby outer slopes of the pre-caldera edifice. The volume of the Myojinsho edifice is estimated to be 2.5–3 km^3, based on the assumptions that the upper 400 m is a simple, free-standing cone and that the deeper part is a cone straddling the pre-existing caldera rim.

Historic activity

Myojinsho is reported to have erupted more than 20 times since 1869. These events are listed and briefly described in Table 1. Care must be taken in interpreting the pre-1952 record, however, for two reasons. Firstly, Myojinsho is now known to be located approximately 9 km ENE of the Bayonnaise Rocks, but the 1896 and 1934 eruptions are said to have taken place 15 km *north* and 10 km *east* of these rocks, respectively. To complicate matters further, Tsukamoto et al. (1990) report that the Bayonnaise Rocks were misplotted by approximately 3 km because of errors on pre-1946 charts. Plotting errors, plus the possibility that eruptions took place from other nearby centers, therefore make the early Myojinsho record suspect. Secondly, Myojinsho was named for the fishing boat (No. 11 Myojin-maru), whose crew first spotted its activity on 17 September 1952 (Morimoto and Ossaka 1955). Prior to that date, the volcano had no name, and all previous activity took place from an unnamed site (or sites) located with respect to the Bayonnaise Rocks. It is possible that the anonymity of the volcano also contributed to confusion and location errors in the historic record.

Judging from its size, Myojinsho doubtless erupted many times prior to 1869, and, given the frequency of its twentieth-century activity, the volcano will probably erupt again.

Table 1 Historic eruptions in the Myojinsho area (Tsukamoto et al. 1990; Simkin and Siebert 1994; Japan Meteorol Agency 1996)

Year	Reported location	Comments
1869	?	Submarine eruption
1870	?	Submarine eruption, new island
1871	?	Submarine eruption
1896	Approximately 8 nautical miles north of Bayonnaisse Rocks	New island forms and then disappears
1906	9 nautical miles northeast of Bayonnaise Rocks	Eruption columns, floating pumice
1915	Approximately 6 nautical miles east of Bayonnaise Rocks	Submarine eruption, eruption columns, discolored water
1934	Approximately 5.5 nautical miles east of Bayonnaise Rocks	Submarine eruption, discolored water, smell of sulfur
1946	31°57′N, 140°01′E	Dome eruption builds new island, which then disappears
1952–1953	Myojinsho	Many explosive eruptions; three cycles of island growth and destruction
1954	Myojinsho	Submarine eruption
1955	Myojinsho	Submarine eruption
1957	Myojinsho	No known eruption, but dead fish found floating nearby
1960	Myojinsho	Submarine eruption; subaerial eruption column rises to 2000–3000 m
1970	Myojinsho	Submarine eruption, discolored water, floating pumice
1971	Myojinsho	Discolored water
1979	Myojinsho	Discolored water
1980	Miyojinsho	Discolored water
1982	Myojinsho	Discolored water
1986	Myojinsho	Discolored water
1987	Myojinsho	Discolored water
1988	Myojinsho	Discolored water

1952–1953 eruption

The 1952–1953 eruption involved three phases of dome growth, each of which formed a small island (or islands), and approximately 1000 phreatomagmatic explosions, which in turn destroyed the domes and repeatedly disrupted the rubbly summit of the volcano. A simplified chronology of the eruption is presented in Table 2; more information is available in Dietz and Sheehy (1954), Morimoto and Ossaka (1955), and Morimoto (1960) and in the many references cited in those reports. Dietz (1954) presented a brief, popularized account of the eruption, accompanied by high-quality photographs. Below, we review selected aspects of the 1952–1953 eruption, concentrating on eruptive and depositional processes.

Table 2 Summary of the 1952–1953 eruption, divided into three stages of dome growth and destruction. Simplified from Morimoto and Ossaka (1955); Niino and Kumakori (1993)

Stage I (most observations made during this stage)	
16 Sept 1952	Eruption (and explosions) begin; tsunamis recorded at Hachijo Island (130 km away); SOFAR signals received in California
17 Sept	Eruption first observed by crew of fishing boat "No. 11 Myojin-maru," whose name was given to the volcano. Numerous small explosions; island emerges from sea
18–23 Sept	Numerous explosions, island persists
24 Sept	Large explosion at 0540 JST; island destroyed. Survey ship No. 5 Kaiyo-maru cruises above submerged volcano summit and is destroyed by large explosion at approximately 12:20 JST
Stage II (intermittent observations only)	
25 Sept–10 Oct	Numerous explosions from submerged volcano summit; eruption columns repeatedly rise into the air
11 Oct	New dome growth builds island
12 Oct–10 March 1953	Numerous explosions; island persists
11 March	Perhaps the largest explosion of the eruption; island is destroyed
Stage III (intermittent observations only)	
12 March–3 April	Numerous submarine eruptions; many subaerial eruption columns noticed
5 April	New island observed
14 April–17 Aug	No explosions observed; island perists
18 Aug–1 Sept	Numerous large explosions; subaerial eruption columns noted; island persists
3 Sept	Continuing explosions; island destroyed; breakers on sea surface mark position of former island
16 Sept–5 Oct	No island visible; minor steaming and discolored water

Dome growth

Domes of hypersthene–augite–dacite emerged above sea level on three occasions during the 1952–1953 eruption. Only the rubbly top of a dome protruded above sea level during September 1952 (Fig. 4A), but larger and more robust domes appeared from early October 1952 to early March 1953 and again from early April to August 1953, forming islands as much as 300 m long. Jagged spines observed in February and April 1953 rose to almost 100 m above sea level (Fig. 4B). The domes were erupted from a vent (or vents) located at Myojinsho's summit at an ocean depth of 50–100 m. Their full dimensions were hidden from view, but they were likely as much as 300–500 m in diameter and 200 m high. Explosions shattered the domes, and the resulting fragments sank quickly and are now contained in deposits mantling the submerged cone. A few fragments were collected, however. Most of these were small (diameter ca. 5 mm) and embedded in floating pieces of wood from the destroyed research ship. Only one "fist-size" piece was recovered; this was found in the bottom of a floating barrel blasted from the deck of the destroyed ship (Morimoto 1960).

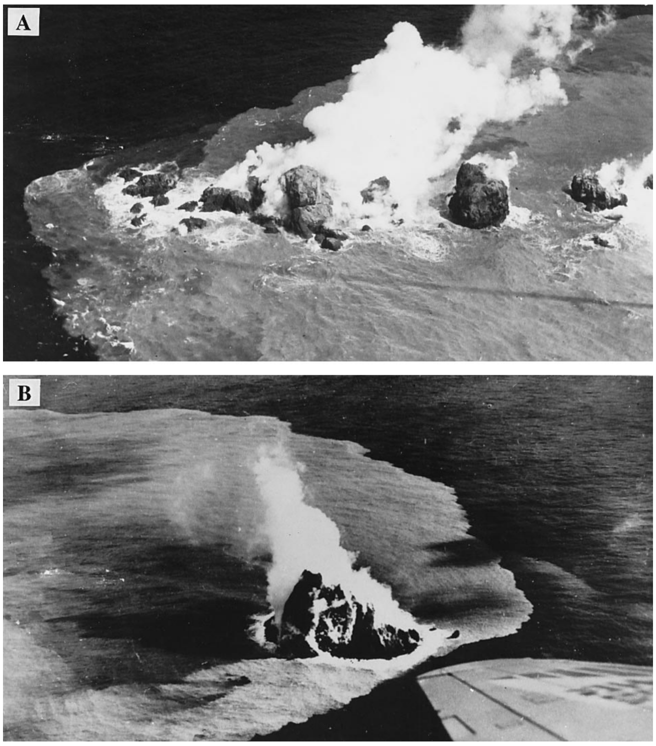

Fig. 4A, B Contrasting appearance of Myojinsho domes visible above sea level. Upwelling plumes of tephra-laden seawater are conspicuous in both photographs. **A** Low, rubbly dome characteristic of the first phase of the eruption. Field of view is approximately 200 m across, north is to the left; photograph by R. Ryan, 22 September 1952. **B** Steep-sided dome and spine protrudes nearly 100 m above sea level. Photograph by U.S. Air Force, 14 April 1953

Explosions

Hundreds of phreatomagmatic explosions occurred during the 1952–1953 eruption. These shattered the dacite domes and likely disrupted adjacent parts of the volcano's summit. The larger explosions involved the eruption of vesiculating magma, forming extensive areas of floating pumice.

The subaerial effects of many dozens of explosions were observed from ships and airplanes. Observers on the Tokyo College of Fisheries' training ship Shinyo-maru obtained sequential photographs of the explosions that began at 08:34 and 13:40 on 23 September 1952 (Morimoto and Ossaka 1955). The explosions, and associated eruption columns, were modest by subaerial standards. A few columns rose to approximately 2 km above sea level (Fig. 5A), and several dozen are known to have been in the 1- 1.5-km range. Some of the more vigorous events displayed the cockscomb pattern reminiscent of the early stages of Surtsey's 1963 activity (Fig. 5B); a few of these produced well-developed surges that traveled outward along the sea surface to distances of a kilometer or more (Fig. 5C). Some explosions took place subaerially, when a dome emerged above sea level to form an island; others were submarine and burst upward through the sea surface. Photographs taken during the earliest stages of two submarine events on 23 September 1952 showed the sea surface to bulge upward just before the explosions burst into the air. The configuration of the water bulges permitted Morimoto and Ossaka (1955) to estimate that these explosions originated at ocean depths of 67 and 41 m, respectively.

The frequency of the explosions, however, was more noteworthy than their size. Most were small and repetitive, sometimes occurring at rates of 3–5 per minute (Morimoto and Ossaka 1955). During the first 11 days of the eruption (16–26 September 1952), when it was most closely observed, sequences of smaller events were punctuated by larger explosions (1–3 each day) that sent eruption columns more than a kilometer above the sea surface. Sensitive receivers of the U.S. Navy's Sofar (Sound Fixing and Ranging) system, approximately 8600 km away in coastal California, detected the sounds of more than 250 explosions during the same 11-day period, confirming the high explosion rates (Deitz and Sheehy 1954). Numerous smaller explosions probably escaped detection.

The volcano was observed less frequently during 1953 than in 1952, and doubtless many explosions were not recorded. In addition, data from the Sofar system were not available for most of 1953, and thus could no longer be used to confirm the scope of the activity. On the basis of the limited data available, however, Mori-

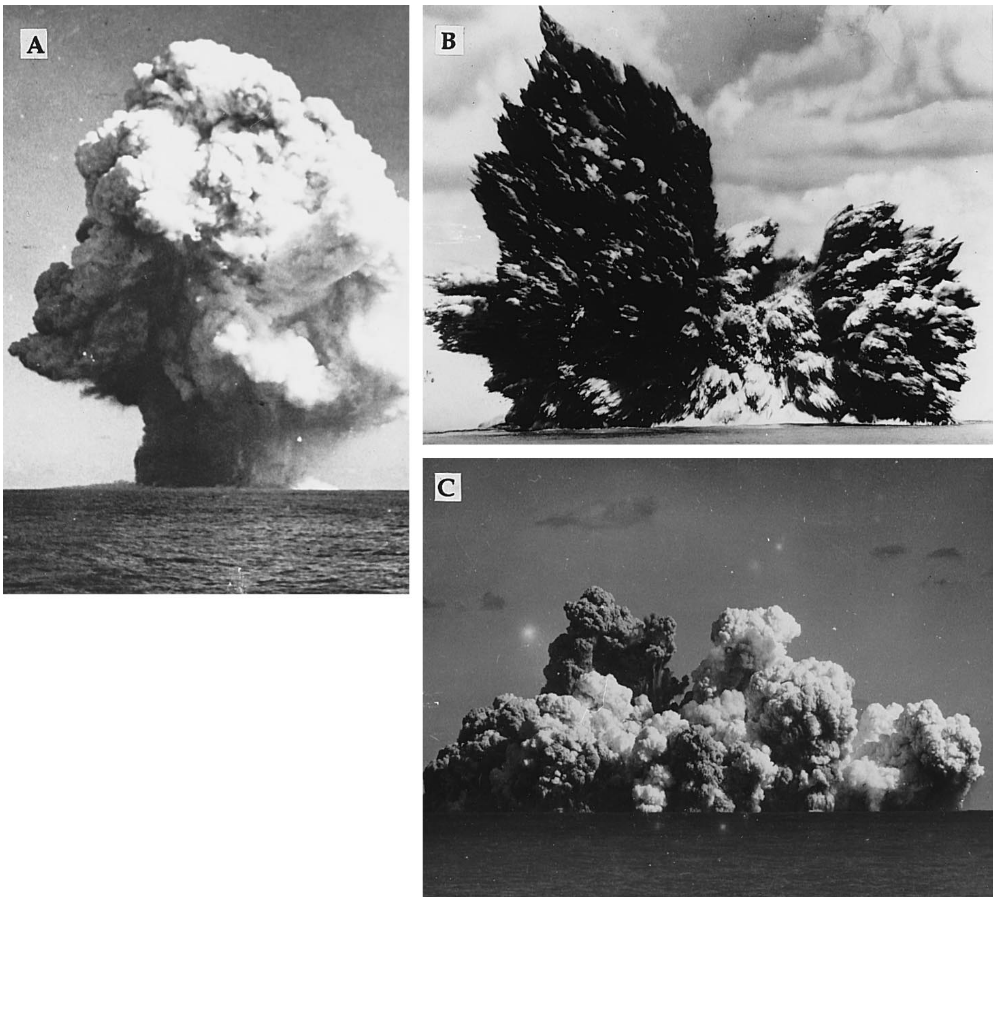

Fig. 5A–C Features of explosive eruptions. **A** Column is approximately 0.8 km wide at its base and 1.8 km high; photograph by S. Murauchi, 08:34 JST, 23 September 1952. **B** Cockscomb pattern accompanies explosion; column is 600 m wide and 400 m high; photograph by A. Shimbun, 13:12 JST, 23 September 1952. **C** Surge travels outward from explosion; column (plus surge) is 1900 m wide and 800 m high; photograph by A. Shimbun, 08:34 JST, 23 September 1952 moto and Ossaka (1955) reported that the explosions of March 1953 were "severe," and that those of late August 1953 were the most destructive of the entire eruption. It is therefore probable that the volcano was just as explosive in March–April and August 1953 as it was in September 1952.

Given the evidence presented above, it is likely that Myojinsho was the site of approximately 1000 explosions during the 12.5-month duration of its 1952-1953 eruption.

Tsunamis

Just one day before the eruption began, a recording wave gauge capable of detecting tsunamis was fortuitously installed on the island of Hachijojima, 130 km north of Myojinsho (Unoki and Nakano 1953). Wave-gauge data for September 1952 (Nakano et al. 1954) document conspicuous tsunamis related to Myojinsho explosions. One tsunami, 92 cm high when it arrived at Hachijojima, took 28 min to travel from Myojinsho to the recording gauge. This wave was triggered by the explosion at 12:20 p.m. on 24 September 1952 that destroyed the survey vessel No.5 Kaiyo-maru. We have been unable to locate tsunami records for the entire duration of the eruption, but Unoki and Nakano (1954) report that approximately 50 waves, believed to have originated at Myojinsho, were recorded at Hachijojima just during 11–25 March 1953. It is therefore possible that hundreds of tsunamis were generated during the explosive phases of activity.

Convective upwelling and dispersal of lapilli and ash

During periods of explosive activity, as well as times of seeming quiescence, conspicuous plumes of discolored water welled to the sea surface above the summit of the volcano and were carried away by near-surface currents (Fig. 4). Plumes of this type are visible in all of the more than two dozen oblique aerial photographs we have examined, and they apparently persisted during all phases of the 12.5-month eruption.

Observers in airplanes and on nearby ships noted the presence of these plumes on many occasions, but few quantitative data were obtained. One ship steamed through the plume approximately 6 km from the volcano's summit on 23 September 1952, and observers reported, "this yellow stream contained much material...as could be judged from the fact that the screw of the ship could be felt to receive the resistance." (Tsuya et al. 1953). They also noted that clear water from beneath the plume welled to the surface in the ship's wake, implying that the plume at that location was relatively thin. At a nearby, but unspecified, location, the same observers collected wire-line water samples through the plume and discovered it to be 25 m thick. Another ship visited the same general area on 21 September 1952, and found that water samples dipped from the near-surface part of the plume were rich in "brown volcanic dust, presumably small fragments of pumice. . . . and a small quantity of pyroxene crystals..." (Nakano et al. 1954). These same workers measured a maximum temperature of 28.0 °C in the surface waters of the plume at a point 5 km from the volcano, approximately 0.5 °C warmer than ambient surface-water temperatures. A temperature anomaly of 0.5-1.0 °C was measured in the water column directly above Myojinsho's summit in May 1989, indicating that the volcano was still emitting substantial amounts of heat (Tsukamoto et al. 1990).

Floating pumice

Most of the tephra erupted from Myojinsho in 1952–1953 likely consisted of dense juvenile debris that quickly sank into the sea. However, conspicuous streaks and patches of floating pumice were noted on numerous occasions. Most of the pumice consisted of lapilli-size clasts, although a few were nearly a meter in diameter and were still hot when hoisted from the water (Tsuya et al. 1953). The fact that these larger clasts did not sink, even though hot, suggests that they cooled in air to such an extent that they were not able to ingest water and sink (e.g., Whitham and Sparks 1986). Several weeks after the disastrous explosion of 24 September 1952, scattered pieces of floating pumice, plus debris from the No. 5 Kaiyo-maru, were observed 600 km southwest of the volcano (Marine Safety Board 1953).

Discussion

Herein we discuss the processes that transported pyroclastic debris to the slopes of the Myojinsho cone and to more distal areas of the surrounding sea floor during the 1952–1953 eruption. Although these inferred processes could not be connected directly to the deposits they produced, because working in the immediate vicinity of the Myojinsho cone is prohibited, both the surface observations and the bathymetry constrain the nature of these processes and how they contributed to cone growth.

Submarine pyroclastic gravity flows

The 1993 bathymetry shows that the upper part of the Myojinsho cone has remarkably uniform slopes. This is well illustrated in the enlargement of the bathymetry shown in Fig. 6A and in the selected profiles in Fig. 6B. In the latter, the volcano's surface in the 300- to 700-m depth range slopes at 21° along each of the five selected transects, indicating this to be the depositional slope on the upper part of the Myojinsho cone. Further downslope, the slope angle gradually decreases to 8–10°, re-

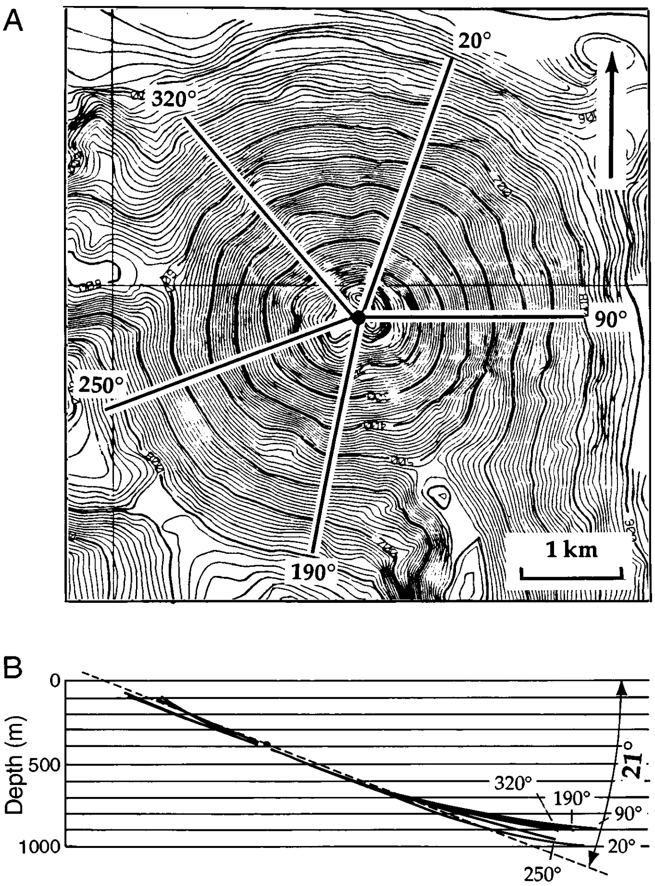

Fig. 6A, B The proximal Myojinsho cone has a remarkably uniform slope of 21° in the depth range 300–700 m. **A** Map view of five Myojinsho profiles; contour interval is 10 m. **B** Five profiles, superposed at 400 m ocean depth

flecting the lower depositional slope of the more distal and deeper deposits. The remarkable symmetry of the cone indicates that the dominant process accounting for edifice growth operated uniformly along all azimuths. We therefore suggest that the shallow-water Myojinsho cone has grown chiefly as a result of deposition from particle flows that traveled downslope along the sea floor, little influenced by wind or the prevailing westerly ocean currents. We use the general term "submarine pyroclastic gravity flows" for these phenomena in order to include a range of gravity flows, including those involving turbidity currents, fluidized beds, grain flows, and debris flows (Lowe 1976, 1982), that likely resulted as both flow velocity and flow density changed during downslope transport. Some single large clasts in these flows may have been hot when deposited (e.g., Kano et al. 1994; Tamura et al. 1991), but, considering that Myojinsho's 1952–1953 eruption was a relatively small, submarine dome-forming event, it is unlikely that the resulting deposits are welded or sintered.

Submarine pyroclastic gravity flows have of course never been observed on Myojinsho's submarine cone, but an indication that they have occurred is provided by a recently acquired sidescan sonar image (Fig. 7). Conspicuous lineations low on the eastern flank of the cone, mostly in the depth range 900–1500 m, are interpreted to be channels and levees formed by the repeated passage of gravity flows. Some of these lineations appear to converge and diverge downslope.

Fallout from air into water and the formation of vertical density currents

Pyroclasts falling from air into water had a variety of dispersal histories. Pumice that cooled in the subaerial eruption columns ingested air, fell to the sea surface, and floated away. Dense juvenile clasts, crystals, and pumice retaining sufficient heat to ingest seawater (cf. Whitham and Sparks 1986; Cashman and Fiske 1991) sank quickly from view, entering water columns 100–400 m deep. Photographs show the subaerial part of the fallout process, but they reveal nothing about what was happening under water.

Although unseen, we suggest that the fallout of pyroclasts through the water column was noteworthy in two respects:

1. The terminal velocity (V_T) of a single particle falling through seawater is approximately one thirtieth that of the same particle falling through air (Fig. 8). Thus, as particles fell from the air into the sea, their V_T abruptly decreased.
2. As particle V_T decreased, their concentration in the water column must have correspondingly increased.

Particle fallout from Myojinsho eruption columns was therefore a two-step process, in which relatively dilute subaerial concentrations were abruptly transformed to dense submarine hyperconcentrations that choked the shallow part of the water column with falling debris. This provided an environment in which gravitational instabilities, leading to the formation of vertical density currents, could play a role in transporting particles to the upper slopes of the volcano.

Conditions for the formation of vertical density currents were first investigated by Bradley (1965), stimulated by his study of diatom sedimentation in lakes. He showed that the settling velocity of particles 10–40 μm in diameter was increased by a factor of ~50 when they fell as dense plumes, rather than separately. Carey et al. (1988) and Druitt (1995) performed tank experiments that confirmed the same effect. Marsh (1988) studied the same general process in the context of the behavior of crystals in magma chambers but scaled the results for application to low Reynolds number conditions (corresponding to dense glassy particles ≤0.3 mm in diameter), where particle accumulation causes density instabilities. He defined conditions for instability by creating a dimensionless number (B) that compares the rate of instability growth (V_i) to the settling rate of a single particle (V_g). The rate of instability growth, V_i, is given by:

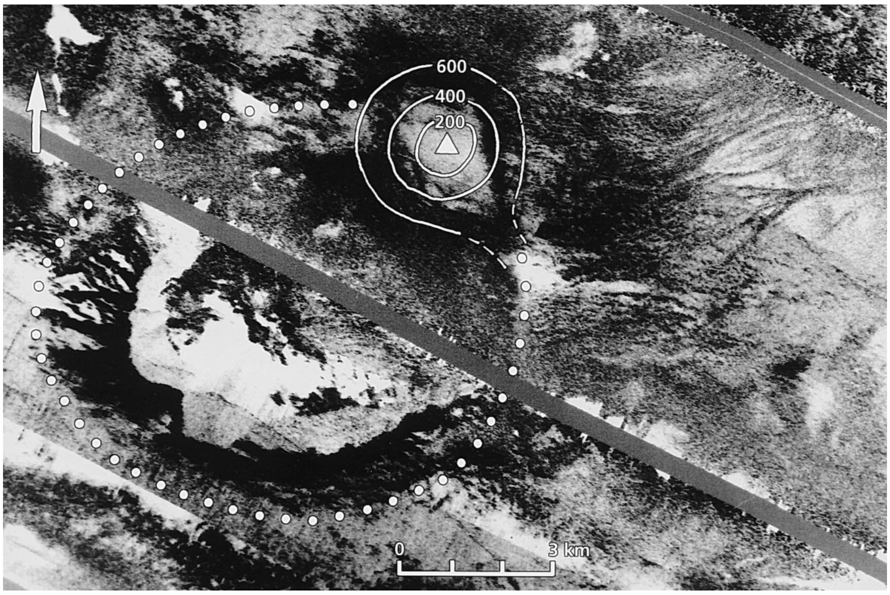

Fig. 7 Sidescan sonar image of the Myojinsho area. Channels and levees, probably formed by submarine pyroclastic gravity flows, form prominent lineaments 3–7 km east of Myojinsho's summit. *White dots* mark the rim of Myojinsho caldera; the diagonal WNW–ESE *stripes* mark the track of the survey ship, along which no image was obtained. (Image kindly provided by. H. Tokuyama, Ocean Research Institute, Univ Tokyo)

$$V_i = C_i\, g h^2 \Delta_i / \mu_i \qquad (1)$$

where h is the layer thickness, μ_i is the viscosity of the fluid, Δ_i, is the density contrast between particle bulk density and the fluid density, and C_i is a constant. The settling rate of a single particle, V_g, is given by:

$$V_g = C_g\, \Delta_g g a^2 / \mu_i \qquad (2)$$

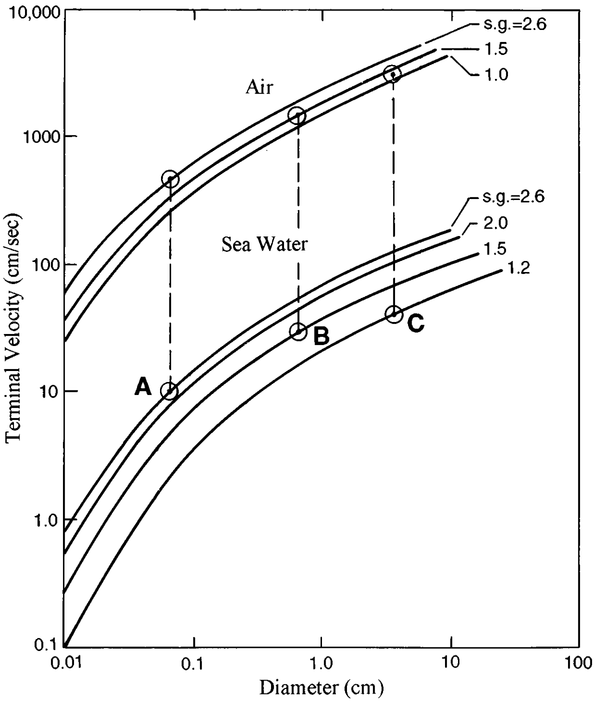

Fig. 8 Terminal velocities of single spheres of differing specific gravity in air and seawater at 20 °C (modified from Cashman and Fiske 1991). Example spheres *A, B,* and *C* have submarine V_T that are less than 3% of their subaerial V_T. This effect causes the particle/fluid ratio in submarine fallout columns to increase by a factor of approximately 30 as particles fall from the air into the sea

where a is the particle radius, Δ_g is the difference between the particle density and the fluid density, and C_g is a shape constant. The two density terms are related, as $\Delta_i = N(\Delta_g)$, where N is the volume fraction of solids in the particle-fluid mixture. Thus, when combined

$$B = V_i/V_g = C\,(h^2/a^2)N \qquad (3)$$

where the constants have been combined to define $C = C_i/C_g$. Vertical density currents will form when $B >> 1$, whereas single-particle settling will dominate for conditions where $B << 1$. Density current formation is generally anticipated for small particle sizes, where, during Stokes flow behavior, V_t increases as the square of particle diameter (e.g., Bradley 1965; Carey et al. 1988). For larger, higher Re particles ($750 \leq Re \leq 10^{5)}$, relevant for clasts having diameters of 2–100 mm falling in seawater (see Cashman and Fiske 1991, Fig. 2), V_t increases only as the square root of particle diameter. Under these conditions, vertical density currents will form when the fraction of solids in aqueous suspension is large (large N) or when the thickness of the particle layer greatly exceeds the average particle radius (large h/a).

Conditions favorable for the formation of vertical density currents clearly existed near the Myojinsho cone, where pyroclasts from subaerial eruption columns repeatedly fell into the sea. Here the dramatic decrease in particle velocity across the air–sea interface would have created high particle concentrations (i.e., large N) in the near-surface water column, which in turn would produce gravitational instabilities leading to the formation of vertical density currents (Eq. (3)). Additional enhancement to the formation of these currents comes from the expected ocean depth of 100–400 m, allowing for potentially large values of h (another means of obtaining large B values), providing a relatively long settling time during which vertical density currents could form. These currents carried particle

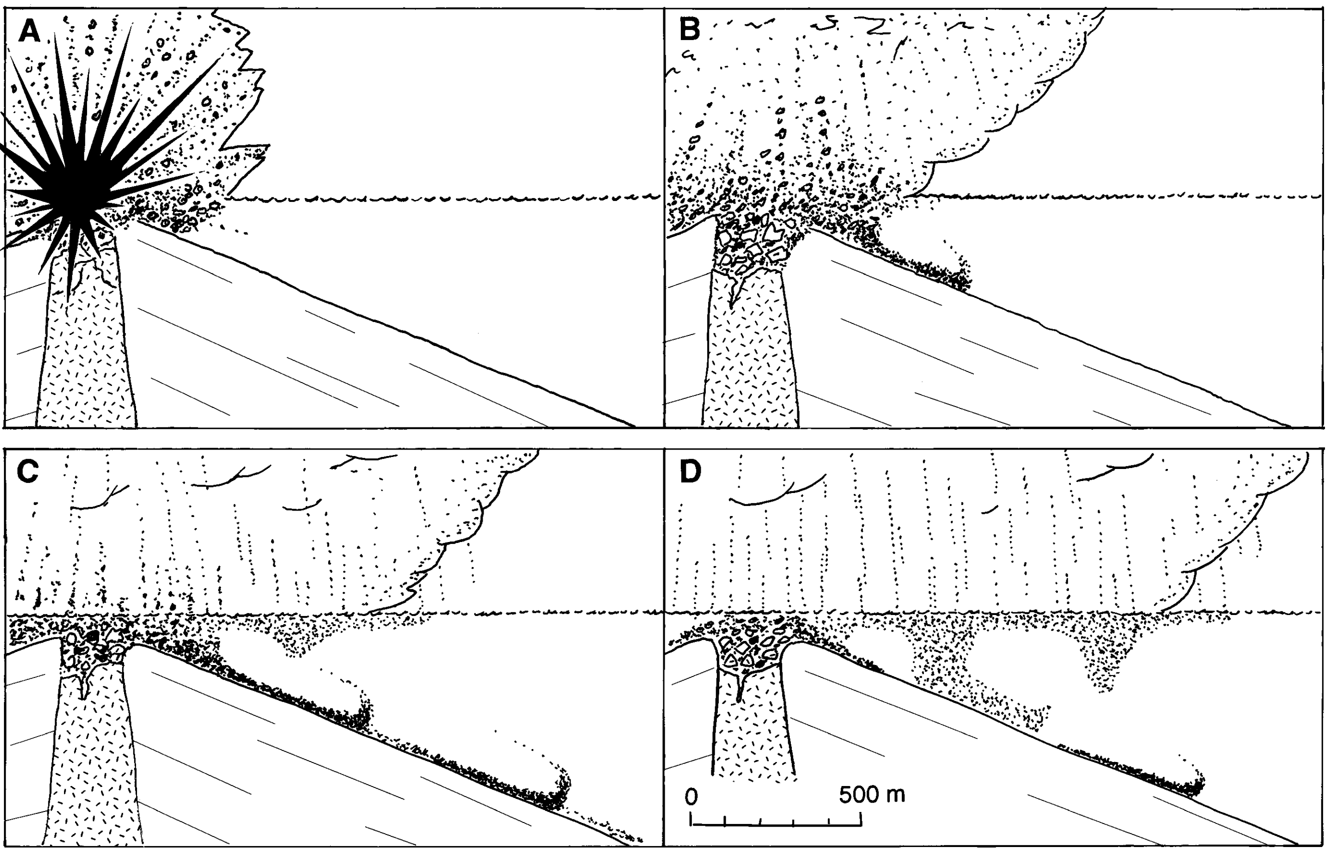

Fig. 9A–D Interpreted transport and deposition of tephra at Myojinsho, 1952–1953. **A** Explosion shatters growing dome, projecting debris upward into the air and sideways into the near-summit water column. **B** Clasts with high terminal velocities (V_T) fall quickly to the volcano's flanks and form submarine pyroclastic gravity flows that travel downslope. **C** Continuing fallout of high-V_T pyroclasts feeds additional pyroclastic gravity flows; subaerial fallout of lower-V_T pyroclasts forms particle hyperconcentrations in near-surface layer. Gravitational instability begins to form inverted plume-like vertical density currents. **D** Vertical density current descends to the volcano's slopes, passing through as much as 400 m of water; the density current continues downslope

hyperconcentrations to the sea floor, and it is likely that, once encountering the 21° slopes of the proximal cone, they continued downslope into deeper water. Thus, there may have been two different flowage phenomena contributing to growth of the Myojinsho cone (Fig. 9): (a) pyroclastic gravity flows, generated directly from explosions and dome collapse and consisting chiefly of coarse, dense debris, that hugged the slopes of the cone; and (b) more dilute density currents, resulting from fallout from subaerial eruption columns, that carried finer-grained pyroclasts down the same slopes. Although admittedly speculative, we suggest that the deposits produced by these more dilute density currents might display features indicative of flowage, such as particle imbrication (e.g., Capaccioni and Sarocchi 1996), as well as those indicative of submarine fallout, such as strongly bimodal pumice-lithic associations (e.g., Cashman and Fiske 1991).

Proximal separation of floating pumice from suspended tephra

After a series of vigorous explosions on 23 September 1952, an accumulation of floating pumice lapilli blanketed the sea surface over a 3×8-km area. The pumice drifted southeastward, in the direction of the prevailing winds, whereas the mass of tephra suspended in the water column separated from the pumice and extended southwestward (Fig. 10). Apparently the floating pumice lapilli that protruded slightly above sea level were influenced by the drag effect of the wind, whereas tephra suspended in the water column was transported only by ocean currents. Because the wind and ocean currents on that day were oriented approximately 90° apart, the floating pumice was abruptly separated from the mass of suspended tephra below. In theory, floating pumice would continue to diverge from suspended tephra until: (a) the pumice became water saturated and sank; (b) the wind velocity decreased to a value much less than that of the ocean current; and/or (c) the wind direction shifted to an azimuth parallel to the ocean currents.

Upwelling plumes

Upwelling plumes of discolored water, often in hues of yellow, green, or "milky blue," are commonly observed on the sea surface above the active submarine volca-

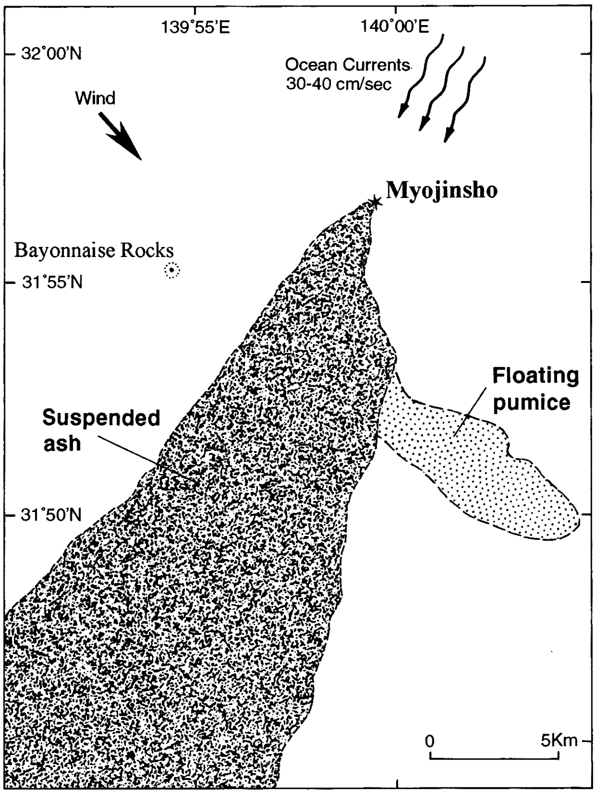

Fig. 10 Contrasting dispersal of suspended ash and floating pumice. Northwesterly winds separated floating pumice from fine tephra suspended in the upper few tens of meters of the water column that drifted southwestward in ocean currents. Observations made from the S.S. Shinyo-Maru following the explosion at 08:34, 23 September 1952. Modified from Fig. 4 of Morimoto and Ossaka (1955)

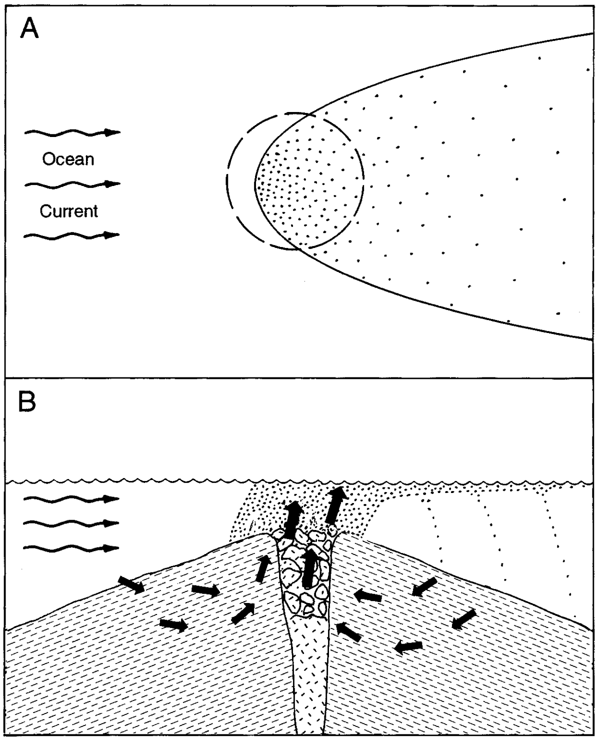

Fig. 11 **A** Plan view and **B** cross section of interpreted convective upwelling at Myojinsho. Seawater is heated as it circulates through hot rubbly debris near the volcano's summit and convects upward, entraining fine particles and carrying them toward sea level. Ocean currents carry the plume away; suspended particles fall slowly to the sea floor over distal areas. The *dashed circle* in **A** outlines the plume origin; ocean currents deflect the plume as it rises toward sea level

noes along the Izu–Ogasawara arc (e.g., at Fukutoku-okanoba on dozens of occasions from 1973 to 1996, as reported in the Smithsonian Institution's Bulletin of the Global Volcanism Network). Some of these plumes may have been associated with submarine eruptions, but others might simply have resulted from the periodic release of heated water that carried fine particles (sublimates and alteration products) toward the sea surface.

At Myojinsho during 1952–1953, however, rising plumes of discolored water were vigorous, persistent, and resulted in an interesting means of long-range pyroclast dispersal. Unlike the episodic submarine suspension of tephra following each of the many explosions, the plumes operated continuously. They are interpreted to be the result of seawater that percolated through the hot, permeable material making up the summit cone. After being heated, the water convected upward, entraining fine tephra as it rose buoyantly toward the sea surface (Fig. 11). Ocean currents carried the plumes downcurrent, and they spread laterally as the heated water (including its load of suspended material) sought its level of neutral buoyancy just below the sea surface. In an equivalent silicic dome eruption on land, inter-eruptive periods are commonly marked only by the gentle release of heated air, steam, and other magmatic gases. In the shallow marine environment, where the ambient fluid (seawater) is significantly denser and more viscous than air, low-V_T pyroclasts can be winnowed from interstices by these rising plumes and made available for downcurrent dispersal.

The detailed functioning of these plumes is intriguing but difficult to quantify. Careful inspection of the plume in Fig. 4A, for example, reveals circular "boils" of upwelling water, indicating that parts of these plumes convected upward at relatively high velocities. If upward velocities of only 50 cm/s were maintained in parts of such plumes (a conservative estimate, we believe, because of the dimensions of these boils), calculated particle fall velocities suggest that dense fragments up to 1 cm in diameter and pieces of pumice 5–8 times larger could be removed from the coarser near-summit deposits and carried to the surface. Once in suspension above the volcano, these particles would be available for lateral transport by ocean currents (Fig. 11). Clasts having higher terminal velocities (V_T) could travel only a short distance laterally before falling to the upper slopes of the cone. Clasts with progressively lower V_T have more gently inclined fall trajectories, and shards and small pumice fragments having very low V_T (<1–2 cm/s, for example) could be carried tens of kilometers away before settling to the sea floor. The total volume of Myojinsho tephra carried distally as a result of convective upwelling is unknown, but it probably comprises a small percentage of the total erupted volume.

We suggest that convective upwelling has at least four important implications:

1. The flushing action of water convecting through the hot rubble at the volcano's summit removes fine-grained matrix, helping to explain the fines-depleted characteristics of similar proximal deposits observed in the geologic record (e.g., Fiske 1986)
2. The removal of matrix likely increases the permeability of the residual proximal deposits, which in turn increases the rate of convective upwelling and improves the efficiency of further matrix removal.
3. The dispersal of fine ash over wide areas by the distal parts of drifting plumes might explain some of the many thin ash layers and ash admixtures found in many deep-sea sediment cores (e.g., Cambray et al. 1995; Fujioka et al. 1992). Thus, instead of representing the products of short-lived explosive events, some deep-sea ash might actually result from convective upwelling at one or more volcanoes that provided a fairly steady supply of fine tephra for months or even years at a time.
4. The combined effect of convective upwelling and fine ash dispersal suggests that care must be taken in interpreting the chemistry of deep-sea tephra layers. Rather than representing a sample of a discrete fallout event (e.g., Straub 1995, 1997), a particular deep-sea tephra layer might actually be the product of convective upwelling that physically mixed a wide variety of particles from one or more source volcanoes. Some of these particles could be related to the ongoing activity, but others could have been swept from the interstices of older unconsolidated deposits. The chemistry of the resulting ash layer might therefore reflect a relatively broad span of magmatic history at the source volcanoes, rather than being representative of closely related magmatic events.

Pyroclast remobilization

There is ample evidence to suggest that secondary pyroclastic gravity flows (i.e., those not the direct product of a pyroclastic eruption) were important in Myojinsho's submarine eruption, much as secondary pyroclastic flows (Torres et al. 1996) and lahars (Pierson et al. 1996) were important in remobilizing tephra following Mount Pinatubo's 1991 subaerial eruption. As described above, many Myojinsho explosions triggered tsunamis, indicating that considerable energy was repeatedly coupled directly into the sea. Because water is an incompressible fluid, the outward motion of seawater accompanying tsunami generation was probably abrupt and disruptive, capable of sweeping large amounts of freshly erupted debris littering the Myojinsho summit both sideways and upward, thus making it available for redeposition. The seismic energy associated with tsunami-generating explosions would also serve to remobilize loose material on the steep slopes of the cone. It would likely be difficult, or even impossible, to distinguish deposits produced as a direct result of explosive eruptions from those produced by the remobilization of temporarily deposited juvenile debris.

The remobilization processes described above could have been further complicated by current action. Strong near-surface currents, particularly the Kuroshiro current (similar to the Gulf Stream in the Atlantic Ocean), frequently affect the Myojinsho area; these currents, traveling at velocities of 0.5–2 m/s and extending to depths of several tens of meters, are probably capable of reworking the pyroclastic debris mantling the uppermost part of the Myojinsho cone. The effects of current action at greater depth are unknown. However, 20 km to the north, at Myojin Knoll caldera, current velocities of 0.3 m/s at a depth of 773 m were measured from a research submersible (R. S. Fiske, unpublished data). It is therefore possible that significant reworking has taken place at depths of several hundred meters.

Conclusion

Myojinsho's shallow marine eruption in 1952–1953 consisted broadly of three episodes of dome growth punctuated by approximately 1000 phreatomagmatic explosions that destroyed the domes and repeatedly disrupted the summit of the volcano. The deposits added to its surface during 1952–1953 consist of some combination of: (a) clasts produced by explosive fragmentation and quench shattering of hot dome rock; (b) autoclastic fragments formed during emplacement and disintegration of domes; (c) remobilized material from previous activity; and (d) water-saturated pumice. The new bathymetric map presented here shows that the Myojinsho cone has slopes of almost exactly 21° in the depth range of 300–700 m. This symmetry suggests that submarine pyroclastic gravity flows, triggered by the explosions, were dominant contributors to cone growth. These flows, traveling down the submarine slopes along all azimuths and little influenced by the prevailing westerly ocean currents, help to explain the cone's remarkable symmetry. The larger explosions produced subaerial eruption columns that showered debris into the sea within 1–2 km of the volcano's summit. Many pyroclasts fell into water columns 200–400 m deep, where their fall velocities abruptly decreased by a factor of ~30. The resulting near-surface particle hyperconcentrations likely spawned vertical density currents that carried pyroclasts to the volcano's slopes at much greater velocities than if they had fallen individually. Some of these density currents may have continued down the volcano's 21° slopes, helping to enlarge the cone. Seawater circulated through the interstices of hot, near-summit debris and convected rapidly upward, entraining fine pyroclasts and forming conspicuous plumes of tephra-laden water that spread out just below the sea surface. These plumes, which persisted for the entire 12.5 months of the eruption, were carried away by near-surface currents and provided a steady supply of fine pyroclasts to the distal sea floor. Perhaps the most fundamental conclusion of this study is that small silicic dome-producing eruptions in shallow water, although intrinsically not very different from similar eruptions on land, disperse pyroclasts into the surrounding environment in ways quite different from their subaerial counterparts.

Acknowledgements This research was funded by the Scholarly Studies Program, Smithsonian Institution (to R. S. F.), the National Science Foundation (grant EAR9418008 to K. V. C.), the Japan Maritime Safety Agency (JMSA), and Mme. Tomo Kikuchi (to R. S. F.). We thank the following people for help and stimulating discussions: K. Iizasa, M. Yuasa (Geological Survey of Japan); H. Furukawa, S. Tani (JMSA); J. Naka (Japan Marine Science and Technology Center); V. Avery, L. Siebert, E. Venzke (Smithsonian Institution); D. Lowe (Stanford University); and T. Ishii, I. Kushiro, Y. Tamura, H. Tokuyama (University of Tokyo). We are indebted to the Asahi Shimbun, the Yomiuri Shimbun, as well as to T. Tiba, H. Foster, C. Siebe, and the late R. Dietz, for help in obtaining photographs. Special thanks are given to S. Oshima, Director General of the Hydrographic Office, JMSA, for continued support and encouragement. We are grateful to R. Cas, P. Kokelaar, and J. McPhie for critically reviewing the manuscript.

References

Bradley WH (1965) Vertical density currents. Science 150:1423–1428

Busby-Spera CJ (1988) Evolution of a Middle Jurassic back-arc basin, Cedros Island, Baja California: evidence from a marine volcaniclastic apron. Bull Geol Soc Am 100:218–233

Cambray H, Pubellier M, Jolivet L, Pouclet A (1995) Volcanic activity recorded in deep-sea sediments and the geodynamic evolution of western Pacific island arcs. In: Taylor B, Natland J (eds) Active margins and marginal basins of the western Pacific. American Geophysical Union, Washington, DC, pp 97–124

Capaccioni B, Sarocchi D (1996) Computer assisted image analysis on clast shape fabric from the Orvieto-Bagnoregio ignimbrite (Vulsini District, central Italy: implications on the emplacement mechanisms. J Volcanol Geotherm Res 70:75–90

Carey SN, Sigurdsson H, Sparks RSJ (1988) Experimental studies of particle-laden plumes. J Geophys Res 93 (15): 314–328

Cas RAF, Landis CA, Fordyce RE (1989) A monogenetic, Surtla-type, Surtseyan volcano from the Eocene-Oligocene Waiareka-Deborah volcanics, Otago, New Zealand: a model. Bull Volcanol 51:281–298

Cashman KV, Fiske RS (1991) Fallout of pyroclastic debris from submarine volcanic eruptions. Science 253:241–352

Dietz RS (1954) The explosive birth of Myojin Island. National Geogr 105:117–128

Dietz RS, Sheehy MJ (1954) Transpacific detection of Myojin volcanic explosions by underwater sound. Bull Geol Soc Am 65:941–956

Druitt TH (1995) Settling behaviour of concentrated dispersions and some volcanological applications. J Volcanol Geotherm Res 65:27–39

Fiske RS (1986) Shallow marine volcanic field in the Mio-Pliocene Shirahama Group, Izu Peninsula, Japan. Geol Soc Am Abstr Prog 18:602

Fiske RS, Naka J (1994) Caldera-forming submarine pyroclastic eruption at Myojin Knoll, Izu-Bonin Arc, Japan. EOS 75:729–730

Fiske RS, Naka J, Iizasa K, Yuasa M (1995) Caldera-forming submarine pyroclastic eruption at Myojin Knoll, Izu-Bonin arc. JAMSTEC J Deep Sea Res 11:315–322

Fujioka K, Nishimura A, Matsuo Y, Rodolfo KS (1992) Correlation of Quaternary tephras throughout the Izu-Bonin areas. Proc Ocean Drilling Prog Sci Results 126:23–45

Houghton BF, Landis CA (1989) Sedimentation and volcanism in a Permian arc-related basin, southern New Zealand. Bull Volcanol 51:433–450

Iizasa K (1993) Assessment of the hydrothermal contribution to seafloor sediments in the Myojinsho submarine caldera, Shichito-Iwojima ridge, Izu-Ogasawara arc, Japan. Mar Geol 114:119–132

Iwabuchi Y, Kato S, Shibata A (1994) The list of volcanoes and their activities records in the adjacent seas of Japan, 2nd edn. Rep Hydrogr Res 30:191–236 (in Japanese with English abstract and figure captions)

Japan Meteorology Agency (1996) National Catalogue of the active volcanoes in Japan, 2nd edn (in Japanese)

Kano K (1996) A Miocene coarse volcaniclastic mass-flow deposit in the Shimane Peninsula, SW Japan: product of a deep submarine eruption. Bull Volcanol 58:131–143

Kano K, Orton GJ, Kano T (1994) A hot Miocene subaqueous scoria-flow deposit in the Shimane Peninsula, SW Japan. J Volcanol Geotherm Res 60:1–14

Lowe DR (1976) Grain flow and grain flow deposits. J Sediment Petrol 46:188–199

Lowe DR (1982) Sediment gravity flows. II. Depositional models with special reference to the deposits of high-density turbidity currents. J Sediment Petrol 52:279–297

Marine Safety Board (1953) Memoir of the investigations on the causes of disaster of the No. 5 Kaiyô-maru (in Japanese)

Marsh BD (1988) Crystal capture, sorting, and retention in convecting magma. Bull Geol Soc Am 100:1720–1737

Morimoto R (1960) Submarine eruption of the Myôjin reef. Bull Volcanol 23:151–160

Morimoto R, Ossaka J (1955) The 1952–1953 submarine eruption of the Myôjin reef near the Bayonnaise rocks, Japan (I). Bull Earthq Res Inst Tokyo Univ 33:221–250

Morimoto R, Fisher RL, Nasu N (1955) Bathymetry and petrography of the Bayonnaise rocks, Japan. Proc Jap Acad 31:637–641

Mueller W (1991) Volcanism and related slope to shallow-marine volcaniclastic sedimentation: an Archean example near Chibougamau, Quebec, Canada. Precambrian Res 49:1–22

Murakami F, Ishihara T (1985) Newly discovered submarine calderas in the northern part of Bonin arc. Earth (Chikyu) 7:637–646 (in Japanese)

Nagaoka S, Okino K, Kato S (1991) Landforms of submarine volcanoes in central part of the Izu-Ogasawara arc, by multibeam sounding system. Rep Hydrogr Res 27:145–172 (in Japanese with English abstract and figure captions)

Naka J, Fiske RS, Taira A, Yamamoto F, Iizasa K, Yuasa M (1995) Geology of Myojin Knoll, Izu-Bonin arc, Japan. JAMSTEC J Deep Sea Res 11:323–331 (in Japanese with English abstract and figure captions)

Nakada J, Fujii T (1993) Preliminary report on volcanic activity at Unzen Volcano, November 1990–November 1991: dacite lava domes and pyroclastic flows. J Volcanol Geotherm Res 54:319–333

Nakada S, Motomura Y, Shimizu H (1995) Manner of magma ascent at Unzen Volcano (Japan). Geophys Res Lett 22:567–570

Nakano M, Unoki S, Hanzawa M, Marumo R, Fukuoka J (1954) Oceanographic features of a submarine eruption that destroyed the Kaiyo-Maru No. 5. Sears Foundation. J Mar Res 13:48–66

Niino H, Kumakori T (1953) Report on the submarine eruption of Myojin-sho. J Tokyo Univ Fisheries 40:1–32

Nishimura A, Rodolfo KS, Koizumi A, Gill J, Fujioka K (1992) Episodic deposition of Pliocene–Pleistocene pumice from the Izu-Bonin arc, leg 126. Proc Ocean Drilling Prog Sci Results 126:3–21

Pierson TC, Daag AS, Delos Reyes PJ, Regalado MTM, Solidum RU, Tubianosa BS (1996) Flow and deposition of posteruption hot lahars on the east side of Mount Pinatubo, July–October 1991. In: Newhall CG, Punongbayan RS (eds) Fire and mud: eruptions and lahars of Mount Pinatubo, Philippines. Univ Washington, Seattle, pp 921–950

Sato H, Fujii T, Nakada S (1992) Crumbling of dacite dome lava and generation of pyroclastic flows at Unzen Volcano. Nature 360:664–666

Simkin T, Siebert L (1994) Volcanoes of the world. Geoscience Press, Tucson

Straub SM (1995) Contrasting compositions of Mariana trough fallout tephra and Mariana Island arc volcanics: a fractional crystallization link. Bull Volcanol 57:403–421

Straub SM (1997) Multiple sources of Quaternary tephra layers in the Mariana trough. J Volcanol Geotherm Res 76:251–276

Swanson DA, Holcomb RT (1990) Regularities in growth of the Mount St. Helens dacite dome 1980–1986. In: Fink JH (ed) Lava flows and domes: emplacement mechanisms and hazard implications. Springer, Berlin Heidelberg New York, pp 3–24

Swanson DA, Dzurisin D, Holcomb RT, Iwatsubo EY, Chadwick WW, Casadevall TJ, Ewert JW, Heliker CC (1987) Growth of the lava dome at Mount St. Helens, Washington (USA), 1981–1983. Geol Soc Am Spec Pap 212:1–16

Takada A, Murakami F, Yuasa M (1994) Geological maps of Aogashima Volcano and submarine volcanoes, south of Izu islands. Geol Surv Japan, 1:10000 geological map

Tamura Y, Koyama M, Fiske RS (1991) Paleomagnetic evidence for hot pyroclastic debris flow in the shallow submarine Shirahama group (upper Miocene–Pliocene), Japan. J Geophys Res 96 (21): 779–787

Tassé N, Lajoie J, Dimroth E (1978) The anatomy and interpretation of an Archean volcaniclastic sequence, Noranda region, Quebec. Can J Earth Sci 15:874–888

Torres RC, Self S, Martinez MML (1996) Secondary pyroclastic flows from the June 15, 1991, ignimbrite of Mount Pinatubo. In: Newhall CG, Punongbayan RS (eds) Fire and mud: eruptions and lahars of Mount Pinatubo, Philippines. Univ Washington, Seattle, pp 665–678

Tsukamoto T, Fukushima H, Kuwakino F, Sakamoto M, Kusunoki K, Oshima S, Kikuchi S (1990) Survey of Myozin-syo using the radio controlled buoy (Manbou). Rep Hydrogr Res 26:45–60 (in Japanese with English abstract and figure captions)

Tsuya H, Morimoto R, Ossaka G (1953) A brief note on the petrography of the pumice ejected from Myojin-sho (reef), near the Beyonnaise rocks, September 23, 1952. J Tokyo Univ Fisheries 40:16–18

Unoki S, Nakano M (1953) On the Cauchy-Poisson waves caused by the eruption of a submarine volcano. Oceanogr Mag 4:119–141

Unoki S, Nakano M (1954) On the Cauchy-Poisson waves caused by the eruption of a submarine volcano (2nd paper). Oceanogr Mag 5:1–13

Whitham AG, Sparks RSJ (1986) Pumice. Bull Volcanol 48:209–223

Yuasa M (1995) Submersible study of Myojin Knoll, northern part of Izu-Ogasawara arc (555). JAMSTEC J Deep Sea Res 11:305–313 (in Japanese with English abstract and figure captions)

Yuasa M, Murakami F, Saito E, Watanabe K (1991) Submarine topography of seamounts on the volcanic front of the Izu-Ogasawara (Bonin) arc. Bull Geol Surv Japan 42:703–743